



HAL
open science

The drosophila Bcl-2 family protein Debcl is targeted to the proteasome by the b-TrCP homologue slimb

Jessie Colin, Julie Garibal, Amandine Clavier, Aurore Rincheval-Arnold, Sébastien Gaumer, Bernard Mignotte, Isabelle Guéna, Isabelle Guenal

► To cite this version:

Jessie Colin, Julie Garibal, Amandine Clavier, Aurore Rincheval-Arnold, Sébastien Gaumer, et al.. The drosophila Bcl-2 family protein Debcl is targeted to the proteasome by the b-TrCP homologue slimb. *Apoptosis*, 2014, 19 (10), pp.1444-1456. 10.1007/s10495-014-1034-8 . hal-02977706

HAL Id: hal-02977706

<https://hal.uvsq.fr/hal-02977706>

Submitted on 26 Oct 2020

HAL is a multi-disciplinary open access archive for the deposit and dissemination of scientific research documents, whether they are published or not. The documents may come from teaching and research institutions in France or abroad, or from public or private research centers.

L'archive ouverte pluridisciplinaire **HAL**, est destinée au dépôt et à la diffusion de documents scientifiques de niveau recherche, publiés ou non, émanant des établissements d'enseignement et de recherche français ou étrangers, des laboratoires publics ou privés.

Apoptosis

The Drosophila Bcl 2 family protein Debcl is targeted to the proteasome by the β -TrCP homologue Slimb --Manuscript Draft--

Manuscript Number:	APPT-D-14-00015R2
Full Title:	The Drosophila Bcl 2 family protein Debcl is targeted to the proteasome by the β -TrCP homologue Slimb
Article Type:	Manuscript
Keywords:	Bcl-2 family proteins; Bax; Debcl; proteasome; Slimb; SCF complex
Corresponding Author:	Isabelle Guéna Université de Versailles st Quentin-en-Yvelines Montigny-le-Bretonneux, FRANCE
Corresponding Author Secondary Information:	
Corresponding Author's Institution:	Université de Versailles st Quentin-en-Yvelines
Corresponding Author's Secondary Institution:	
First Author:	Jessie Colin, PhD
First Author Secondary Information:	
Order of Authors:	Jessie Colin, PhD
	Julie Garibal, PhD
	Amandine Clavier
	Aurore Rincheval-Arnold, PhD
	Sébastien Gaumer, PhD
	Bernard Mignotte, PhD, Professor
	Isabelle Guéna
Order of Authors Secondary Information:	

1 **The Drosophila Bcl-2 family protein Debel is targeted to the proteasome by the β -TrCP**
2 **homologue Slimb**
3

4 Jessie Colin, Julie Garibal, Amandine Clavier, Aurore Rincheval-Arnold, Sébastien Gaumer, Bernard Mignotte
5 and Isabelle Guénal
6

7 Laboratoire de Génétique et Biologie Cellulaire, EA4589, Université de Versailles Saint-Quentin en Yvelines,
8 Ecole Pratique des Hautes Etudes, Bâtiment Simone Veil, 2 avenue de la Source de la Bièvre, 78180 Montigny-
9 le-Bretonneux, France
10

11
12
13
14 **Corresponding author:**

15 Dr Isabelle GUENAL
16 Laboratoire de Génétique et Biologie Cellulaire, EA 4589,
17 Université de Versailles Saint-Quentin-en-Yvelines,
18 Ecole Pratique des Hautes Etudes,
19 Bâtiment Simone Veil
20 2 avenue de la Source de la Bièvre
21 78180 Montigny-le-Bretonneux
22

23
24 Tel: + 33 (0)1 70 42 94 36
25 e-mail: isabelle.guenal@uvsq.fr
26

27
28 **Keywords : Bcl-2 family proteins; Bax; Debel; proteasome; Slimb; SCF complex**
29
30
31
32
33
34
35
36
37
38
39
40
41
42
43
44
45
46
47
48
49
50
51
52
53
54
55
56
57
58
59
60
61
62
63
64
65

Abstract:

The ubiquitin-proteasome system is one of the main proteolytic pathways. It inhibits apoptosis by degrading pro-apoptotic regulators, such as caspases or the tumor suppressor p53. However, it also stimulates cell death by degrading pro-survival regulators, including IAPs. In *Drosophila*, the control of apoptosis by Bcl-2 family members is poorly documented. Using a genetic modifier screen designed to identify regulators of mammalian *bax*-induced apoptosis in *Drosophila*, we identified the ubiquitin activating enzyme Uba1 as a suppressor of *bax*-induced cell death. We then demonstrated that Uba1 also regulates apoptosis induced by Debcl, the only counterpart of Bax in *Drosophila*. Furthermore, we show that these apoptotic processes involve the same multimeric E3 ligase — an SCF complex consisting of three common subunits and a substrate-recognition variable subunit identified in these processes as the Slimb F-box protein. Thus, *Drosophila* Slimb, the homologue of β -TrCP targets Bax and Debcl to the proteasome. These new results shed light on a new aspect of the regulation of apoptosis in fruitfly that identifies the first regulation of a *Drosophila* member of the Bcl-2 family.

Introduction

The ubiquitin-proteasome system (UPS) is one of the main proteolytic pathways in the cell. Ubiquitination requires three specialized enzyme families. The first step of ubiquitination involves a ubiquitin activating enzyme called E1, which covalently binds a ubiquitin monomer. This activated ubiquitin is transferred to a ubiquitin conjugating enzyme, E2. A ubiquitin ligase (E3) then catalyzes the transfer of ubiquitin to a specific target. A broad diversity of E3 ligases exists, to cope with the very large number of substrates of the UPS. E3-dependent polyubiquitination of the substrate can lead to its recognition by the proteasome — a macromolecular complex responsible for the degradation of ubiquitin-tagged proteins into short peptides. The UPS controls many processes such as the cell cycle or apoptosis by targeting some of their main regulators.

In mammals, members of the Bcl-2 family are key elements of the apoptotic machinery (review : (1)). This multigenic family has about 20 members, which may either promote or inhibit apoptosis. Members of the Bcl-2 family control cell death either by inhibiting or promoting mitochondrial outer membrane permeabilization. This permeabilization is a key step in the execution of the mitochondrial apoptotic pathway in mammals, as it allows the release of apoptogenic factors, such as cytochrome c, from the mitochondrion into the cytosol. This cytochrome c release is essential for Apaf-1-mediated caspase-9 activation and cell breakdown.

One of the best described examples of the UPS regulation of Bcl-2 family members-induced cell death in mammals is provided by the degradation of the anti-apoptotic protein Mcl-1. Three E3 ligases have been shown to target Mcl-1 for degradation *via* two independent pathways. The first of these enzymes, Mule (Mcl-1 ubiquitin ligase E3) is a HECT domain-containing E3 ligase (2). It contains a BH3 domain, also found in members of the Bcl-2 family, which mediates the physical interaction between Mule and Mcl-1. Mcl-1 can also be downregulated by phosphorylation on two serine residues by GSK-3 β (glycogen synthase kinase-3 β). This hyperphosphorylation of Mcl-1 leads to its recognition by the F-box protein β -TrCP (3). β -TrCP acts within a multimeric RING domain-containing E3 ligase, called SCF complex. The F-box protein is a variable subunit of this complex responsible for substrate recognition, leading to ubiquitination by the SCF complex and subsequent degradation by the proteasome. More recently, it has been shown that Trim17-mediated ubiquitination and degradation of Mcl-1 initiate apoptosis in neurons (4). Other members of the mammalian Bcl-2 family are regulated in a proteasome-dependent manner. Such regulation has been demonstrated for anti-apoptotic proteins, such as Bcl-2 (5), and pro-apoptotic proteins, such as Bid (6) and Bim (7). However, the precise mechanisms underlying this regulation, including the post-translational modifications targeting them for UPS-mediated degradation, and the identity of the E3 ubiquitin ligases involved remain unclear.

Bax, a multidomain pro-apoptotic member of the Bcl2 family, is a target of the UPS (8, 9). Some evidence suggest that the signal for Bax degradation could be the Akt-mediated phosphorylation of serine 184 (10-13) and that the DNA repair protein Ku70 could be involved in Bax deubiquitination (14). However, the ubiquitin ligase responsible for Bax targeting to the proteasome as well as the regulation of this degradation pathway remain to be characterized.

Only two members of the Bcl-2 family have been identified in *Drosophila* so far, Buffy and Debcl. Both display a mitochondrial subcellular localization and are apoptotic regulators, suggesting that mitochondria play an important role in apoptosis in *Drosophila*. Buffy was originally described as an anti-apoptotic Bcl-2 family member (15, 16), but in some cases it can promote cell death (17-20). Debcl (death executioner Bcl 2 homolog), is a multidomain death inducer (20-24) that can be inhibited by direct physical interaction with Buffy (15). When overexpressed in mammalian cells, Debcl induces both cytochrome c release from mitochondria and apoptosis. This protein interacts physically with anti-apoptotic members of the Bcl 2 family, such as Bcl 2 itself, in mammals. Debcl is involved in the control of some developmental cell death processes as well as in the irradiation response (16, 19, 25).

1 Most apoptotic processes in *Drosophila* involve the initiator caspase Dronc and its adaptor Dark (26).
2 Dronc activation is tightly controlled by Diap1. Indeed, loss-of-function mutations in *diap1* are often sufficient
3 to induce apoptosis (27-29). Diap1 has been widely studied and acts as an E3 ubiquitin ligase, targeting caspases,
4 including Dronc, for proteasomal degradation. Diap1 is itself targeted for proteasomal degradation in response to
5 pro-apoptotic RHG (Rpr, Hid, Grim) protein signaling. Therefore, the UPS plays a key role in regulating
6 apoptosis in *Drosophila* by acting on caspases, IAPs or RHG proteins. However, no data are available
7 concerning the degradation of *Drosophila* Bcl-2 family members by the proteasome and the mechanisms of
8 action and regulation of Debcl and Buffy remain poorly documented as compared to our knowledge of their
9 mammalian counterparts (30).

10 Therefore, we investigated the roles of Bcl-2 family members in *Drosophila*, using transgenic flies
11 expressing the murine *bax* gene under control of the inducible UAS/Gal4 system (31). We have previously
12 shown that mammalian Bax is functional in *Drosophila* where it interacts with the cell death machinery to
13 induce an apoptosis involving mitochondrial events (32, 33). We have also shown that *bax*-induced apoptosis
14 can be antagonized in *Drosophila* by overexpressing mammalian *bcl-2* (31, 32). Studies of *debcl* demonstrated
15 that both *debcl*- and *bax*-induced cell death share common features. Indeed, the mitochondrion stands as a key
16 component of *debcl*- and *bax*-induced apoptosis and both trigger two different cell death pathways. The first one
17 is effector caspase-dependent while the second appears to resist p35 inhibition, suggesting the existence of an
18 effector caspase-independent pathway. *Bax*- and *debcl*-induced apoptosis in the wing disc result in a wing
19 phenotype and partially penetrant fly lethality. To identify suppressors of *bax*- and *debcl*-induced cell death, we
20 screened a library of gain-of-function mutants (34) for modifiers of these phenotypes (Colin *et al.*, in
21 preparation). One of the suppressors identified this way consists in a mutation of the gene encoding the unique
22 ubiquitin activating enzyme, *Uba1*. Studies of this mutant provided insight into the proteasome-dependent
23 regulation of Bcl-2 family members in *Drosophila*. We show here that Bax and its counterpart Debcl are
24 degraded by the proteasome in *Drosophila*. We identified the E3 ubiquitin ligase Slimb (*Slmb*), the *Drosophila*
25 homologue of β -TrCP, as the regulator of Debcl levels.

26 27 28 **Materials and methods**

29 30 **Fly stocks**

31 Flies were raised on standard medium at 25°C, except those used for phenotypic suppression tests
32 involving *vg>bax* flies, which were performed at 18°C. *UAS-bax* flies were generated in our laboratory. The *yw^c*,
33 *w¹¹¹⁸*, *vg-gal4*, *hs-gal4* and *da-gal4* strains are described in (31, 32). *ptc-gal4* flies were provided by L.
34 Théodore. *UAS-debcl-HA* flies were generously provided by H. Richardson (35). The *slmb* mutants *slmb⁸* and
35 *slmb⁴¹* were generously provided by B. Limbourg-Bouchon (36). The *UAS-slmb^{DN}-flag-myc* flies were
36 generously provided by T. Murphy. In this strain, the *UAS-slmb^{DN}* transgene expresses dominant-negative Slmb
37 protein containing five point mutations in the F-box domain that completely abolish interaction with SkpA, and
38 includes a 3xFLAG-6xmyc N-terminal epitope made with the pTFMW vector (Drosophila Genomics Resource
39 Center; T.D. Murphy, personal communication). *Uba1^{UY3010}* was generated by mobilizing *P[Mae-UAS.6.11]*
40 (*P[UY]*). *Uba1^{EP2375}*, *morgue^{EP1184}* and *pros25^{EP931}* were obtained from Szeged Stock Center. *Uba1^{s3484}* and
41 *skpA^{EP1423}* were obtained from Bloomington Stock Center. The *Ap54* mutant described by T. Szlanka (37) was
42 generously provided by A. Udvardy. *UAS-PABP-flag* flies (#9420) were obtained from Boomington.

43 44 45 **Wilcoxon test**

46 *vg>bax*, *vg>rpr* and *ptc>(debcl)₂* virgins were crossed, in parallel, with the tested mutant and a control
47 strain. We have previously verified that the presence of a *UAS-GFP* transgene does not affect *bax*- or *debcl*-
48 induced phenotypes (data not shown). Therefore, there is no detectable GAL4 titration in our system. Thus,
49 according to the genetic background of the tested mutant strains, control experiments were performed by
50 crossing *vg>bax* or *ptc>Debcl* females with *w¹¹¹⁸* males, except for the *UY³⁰¹⁰* mutant strain for which *ywc*
51 males were used. The progenies of each of these crosses were classified, according to the strength of the wing
52 phenotype, into four phenotypic categories (from wild-type to strong phenotype) by the same blind observer to
53 avoid changes in categorization. A Wilcoxon test was then used to compare the distributions of phenotypes
54 between the two lineages (T: test *versus* C: control). Differences in distribution were considered significant if α
55 $< 10^{-3}$. A positive *Ws* value indicates enhancement of the phenotype and a negative *Ws* value indicates
56 suppression of the phenotype.

Identification of the *P[UY]* insertion in the *UY3010* mutant

For identification of the gene affected in the *UY3010* mutant, we used inverse PCR and sequencing of the DNA flanking the *P[UY]* element. Inverse-PCR was carried out as in the BDGP protocol (<http://www.fruitfly.org/about/methods/inverse.pcr.html>). We used genomic DNA from young *UY3010* males and *MspI* for DNA digestions. The following primers were used: 5'-GCTTTCGCTTAGCGACGTGT-3', 5'-CAGATCGTAAGGGTTAATGTT-3', 5'-GAATTGAATTGTCGCTCCGT-3', and 5'-CTCTCAACAAGCAAACGTGC-3'.

Immunostaining

Wing discs were dissected from *vg>bax* or *vg>bax/Uba1^{EP2375}* third-instar larvae in PBS, pH 7.6 and fixed in 3.7% formaldehyde. Discs were labeled by incubation for 2 hours with anti-Bax $\Delta 21$ antibody (1/200) in 0.3% Triton X-100/10% NGS in PBS (PBT/NGS). After washing in 0.3% Triton X-100 in PBS, TRITC-conjugate was incubated for 1 hour in PBT/NGS. Images were captured with a conventional Leica DMRHC research microscope, using an N2.1 filter to detect TRITC fluorescence. The same exposure time was used for all images.

Immunoprecipitation

Two hundred embryos were collected, dechorionated in 100% sodium hypochlorite and rinsed in PBS. Embryos were then collected by centrifugation and washed once in PBS. Pellets were resuspended in 270 μ l of ice-cold CHAPS buffer (10 mM Hepes pH 7.4, 150 mM NaCl, 1% CHAPS, 1 mM DTT, Pefabloc) and homogenized on ice with a Wheaton glass homogenizer (until the suspension became milky). For control immunoprecipitation, 75 μ l of lysate was incubated 4 hours at 4°C with 3 μ g of IgG1 before the addition of 15 μ l of protein G-agarose beads overnight at 4°C. For anti-Slmb immunoprecipitation, 75 μ l of lysate was incubated overnight at 4°C with 5 μ l of anti-FLAG M2 agarose beads (Sigma Aldrich). Immune complexes were then washed four times with ice-cold CHAPS buffer and resuspended in loading buffer. Samples were boiled for 5 min. and proteins were subjected to western blotting as described below.

Western blot

Western blotting was carried out with the INVITROGEN NuPAGE™ system according to the manufacturer's instructions, with 4 to 12% Bis-Tris Gels and MES running buffer (50 mM MES, 50 mM Tris base, 0.1% SDS, 1 mM EDTA, pH 7.3). Proteins were electrotransferred onto PVDF membrane (Immobilon™-P, MILLIPORE) in transfer buffer (25 mM Bicine, 25 mM Bis-Tris, 1 mM EDTA, pH 7.2). Transfer efficiency was evaluated with Ponceau-S (0.3% Ponceau-S, 1% acetic acid). Membranes were saturated by incubation for one hour with skim milk before antibody staining.

Antibodies

Immunostaining was performed with anti-Bax $\Delta 21$ (Santa Cruz, 1/200) and TRITC-conjugate anti-rabbit (Jackson, 1/200) antibodies. Western blots were probed with anti-Bax 5B7 or N20 (Santa Cruz, 1/500 or 1/200 respectively), anti-HA (Babco, 1/1000), and anti-tubulin E7 (DSHB, 1/1000) antibodies. HRP-conjugate anti-mouse or anti-rabbit antibodies were obtained from Jackson Laboratories and used at a dilution of 1/10000. Immunodetection was performed by a chemoluminescence-based method (ECL, Amersham).

In Situ Proximity Ligation Assay (PLA)

Ptc>Debcl-HA, Slmb^{DN}-flag-myc and *Ptc>Debcl-HA, Pabp-flag* third instar larvae were dissected in PBS pH 7.6, fixed in PBS/formaldehyde 3.7%, washed three times for 5 min in PBT (PBS, 0.3% Triton). Wing imaginal discs were then dissected and incubated in PBT/FCS (PBS, 0.3% Triton, 10% FCS) at room temperature during 20 min. *In situ* PLA was performed using the Duolink® kit (Olink Bioscience) essentially according to manufacturer's instructions. Briefly, wing imaginal discs were stained with primary antibodies overnight at 4°C. The antibodies used for Duolink assays and their corresponding dilutions are: anti-HA antibody (ab9110, abcam®, 1/200) and anti-flag.M2 antibody (Agilent, 1/200). After washing, wing imaginal discs were incubated with the secondary oligonucleotide-linked antibodies (PLA probes: anti-Mouse PLUS and anti-Rabbit MINUS) provided in the kit. The oligonucleotides bound to the antibodies were hybridized, ligated, amplified, and detected using a fluorescent probe (Detection Kit 563). Discs were mounted in Citifluor™ (Biovalley) and observed with a Leica SP2 upright confocal microscope.

Results

Isolation of the *UY3010* mutant

The expression of mammalian *bax* during development using the *vg-gal4* driver — which targets expression to the wing margin tissue — led to an apoptosis-induced variable notch phenotype in the adult wing (figure 1A-D and (31, 32)). Moreover, this excess of apoptosis led to an increase in fly lethality. We used these phenotypes to screen the mutants of the *P[UY]* collection (34), which present a random insertion of a UAS-containing *P*-element. Out of the 1475 tested mutants, only 17 modifier genes suppressing *bax*-induced apoptosis were identified, showing how stringent our screen was. One of the suppressors we identified was the *UY3010* mutation. This mutation attenuated both the wing phenotype and lethality due to *bax* expression and did not display any phenotype in absence of *bax* when driven by *vg-gal4* or *ptc-gal4* (data not shown). We carried out a phenotypic suppression test, validated by the statistical Wilcoxon test (see Materials & Methods) to confirm the suppressor effect of this mutation. The result of this phenotypic suppression test is presented figure 1E. In the control cross offspring (*Uba1^{UY3010}C*), expressing only *bax*, only 3.4% of the progeny displayed a weak phenotype. The percentage of weak phenotypes increased to 41% of the progeny in the test cross (*Uba1^{UY3010}T*), in which flies expressed *bax* in presence of the *UY3010* mutation. The Wilcoxon test gave a probability of 5×10^{-15} for this shift, which is highly significant ($\leq 10^{-3}$). We conclude that the *vg-gal4*-mediated induction of the *UY3010* mutation significantly suppresses the *bax*-induced phenotype.

Characterization of the *Uba1^{UY3010}* allele

We carried out inverse PCR on genomic DNA from *UY3010* flies to identify the genes flanking the *UY3010* insertion. We sequenced the PCR products and localized the *P[UY]* insertion to the 5'UTR region of the E1 ubiquitin activating enzyme gene, *Uba1*. The *P[UY]* was found to be inserted 258 bp upstream from the translation initiation codon and 554 bp downstream from the transcription start site in an orientation compatible with *Uba1* overexpression in the *UY3010* mutant in the presence of *gal4* (supplementary figure 1).

We checked whether *gal4* induction led to *Uba1* overexpression in the *UY3010* mutant, using the *hs-gal4* driver to trigger the *UAS*-dependent transcription of *Uba1* (supplementary figure 2). As expected, *Uba1* transcript levels present a 40 fold increase in heat shocked *hs>Uba1^{UY3010}* flies compared with *Uba1^{UY3010}* or wild type flies, showing that the *UY3010* mutation leads to *UAS/Gal4*-dependent *Uba1* overexpression.

We investigated whether this overexpression led to synthesis of a functional form of the *Uba1* protein. Thus, we tested its ability to complement the null allele *Uba1^{s3484}*. The progeny of a genetic cross between flies carrying the *UY3010* mutation and *Uba1^{s3484}* flies, did not count any *Uba1^{s3484}/Uba1^{UY3010}* flies (table 1), showing that in the absence of *Gal4* the *UY3010* allele is a loss of function. In contrast, ubiquitous induction of *Uba1* using the *da-gal4* driver rescued heterozygous *Uba1^{s3484}/Uba1^{UY3010}* flies. Besides, we observed that decreasing *Uba1* levels thanks to a background heterozygous for the *Uba1^{s3484}* null allele failed to modify *bax*-induced phenotypes (data not shown). Altogether, these data demonstrate that *UY3010*-mediated suppression of *bax*-induced phenotypes is due to overexpression of a functional form of *Uba1*.

Uba1 overexpression abolishes *bax*-induced apoptosis

The *UY3010* mutant was isolated based on its ability to suppress *bax*-induced phenotypes. We tried to reproduce this suppression by overexpressing *Uba1* with another allele reported to overexpress *Uba1* in a *gal4*-dependent manner, the *Uba1^{EP2375}* allele (38). This allele presents a *UAS*-containing *P*-element different from *P[UY]* but inserted in the same region. We verified that driving expression of *Uba1^{EP2375}* using *vg-gal4* or *ptc-gal4* did not lead to any wing phenotype. The *Uba1^{EP2375}* allele allowed a much stronger suppression of the *bax*-induced phenotype than *Uba1^{UY3010}*. The *Uba1^{UY3010}* allele gave weak phenotypes in about 40% of cases, but never gave rise to wild-type wings or wings with only a very small notch. By contrast, as shown in figure 2A, B and C, *Uba1^{EP2375}* gave mostly very weak phenotypes (wings with only a very small notch in the posterior region of the wing margin) and wild-type wings. Thus, *Uba1* overexpression from the *Uba1^{EP2375}* allele abolished the notched wing phenotype almost totally. This stronger suppression indicates that this allele may produce more *Uba1* protein than *Uba1^{UY3010}*.

As previously described, *bax* expression induced apoptosis and an alteration of wing disc morphology (figure 2D-E and (32)). To test whether *Uba1* suppression of *Bax*-induced wing phenotypes is associated to a decrease of cell death, we stained apoptotic cells with acridine orange (AO) in third instar larvae imaginal discs. The number of apoptotic cells was strongly reduced when *Uba1* was co-expressed with *bax* (figure 2F-G).

We chose to express *bax* in the wing disc from the *vg-gal4* driver, because *Bax* is such a potent death inducer that most *gal4* drivers induce massive apoptosis leading to the embryonic death as observed with the ubiquitous *da-gal4* driver (31, 32). As *Uba1* overexpression efficiently suppresses *bax*-induced phenotypes, we tried to prevent *bax*-induced lethality by overexpressing the *Uba1^{EP2375}* allele with the *da-gal4* driver. This resulted in the survival of part of the offspring despite the ubiquitous overexpression of *bax* (data not shown).

Thus, *Uba1* overexpression inhibits the massive wave of apoptosis induced by *bax*, allowing embryos to develop to adulthood.

***Uba1* overexpression suppresses *debcl*-induced cell death**

Little is known about *Debcl* regulation in fruit flies and we decided to investigate whether *debcl*-induced cell death was also sensitive to *Uba1* overexpression. We carried out a phenotypic suppression test with *debcl*-expressing flies. Ectopic *debcl* expression in the wing disc with the *ptc-gal4* driver induced apoptosis along the antero-posterior frontier (supplementary figure 3). In adult wings, this apoptosis led to the L3 and L4 veins being brought closer together in the proximal region of the wing and the fusion of these veins at the anterior crossvein (figure 3B-B'). *Uba1*^{EP2375} allele overexpression almost completely abolished this phenotype (figure 3C-C') and increased the percentage of wild-type phenotypes from 0 to 80% (figure 3H).

Uba1^{UY3010} expression did not significantly suppress *debcl*-induced phenotypes ($\alpha=1.8 \times 10^{-3}$). However, *Uba1*^{EP2375} gave efficient phenotypic suppression of *debcl*. The difference in the results obtained with these two alleles could lie in the *Uba1* protein overproduction capacity of the two constructs. However, RT-qPCR did not reveal any significant difference between the *Uba1* mRNA levels observed in *Uba1*^{UY3010} and *Uba1*^{EP2375} strains (data not shown), possibly as the consequence of a limited number of cells expressing Gal4 in the imaginal disc when using a *ptc* driver. Nevertheless, these results show that *Uba1* overexpression inhibits the apoptotic processes induced both by *Bax* or *Debcl*.

Proteasome activity modulates *bax*- and *debcl*-induced apoptosis

We have shown that *Uba1* overexpression inhibits the apoptosis induced by *bax* or *debcl*. Therefore, we investigated the possible role of the proteasome in the regulation of *bax*- and *debcl*-induced cell death, by modifying proteasome activity and assessing the effects of these modifications on apoptotic processes. We carried out phenotypic suppression tests, using mutants with defective proteasomal subunits. We chose to use the $\Delta p54$ mutant, as this mutant has been well characterized (37) and displays no wing phenotype. It carries a deletion of the *p54/S5a/Rpn10* gene, which encodes a subunit of the 19S regulatory particle of the proteasome. This subunit links the base and lid subcomplexes of the 19S regulatory particle. It also acts as a "receptor" for the 26S proteasome by interacting with polyubiquitin chains. Szlanka *et al.* have shown that deletion of *p54* in *Drosophila* activates a regulatory feedback loop, leading to 26S proteasome overexpression (37). We used this mutant to increase proteasomal activity with this mutant. We also used the *pros25*^{EP931} loss of function allele that carries a mutation affecting negatively the $\alpha 2$ subunit of the 20S core particle of the proteasome and does not lead by itself to any phenotype when driven by *vg-gal4* or *ptc-gal4*. We assessed the effects of these mutations on proteasome activity, by western blot analysis of the degradation of Armadillo, a known target of the proteasome (Supplementary figure 4). As expected, the $\Delta p54$ mutant stimulated the proteasomal activity whereas the *pros25*^{EP931} allele inhibited proteasomal activity (39).

The $\Delta p54$ mutation shifted the distribution of *bax*-induced phenotypes toward weaker phenotypes (figure 4, compare $\Delta p54C$ and $\Delta p54T$). Indeed, the progeny of the control cross included 49.5% strong phenotypes and only 0.5% weak phenotypes, whereas crosses with the $\Delta p54$ mutant gave 4.9% strong phenotypes and 45.7% weak phenotypes. By contrast, *pros25*^{EP931} shifts the phenotypic distribution toward stronger phenotypes, doubling the percentage of strong phenotypes with respect to the control cross (figure 4 compare *pros25*^{EP931} C and T). We can therefore conclude that enhancing the proteasomal activity suppresses *bax*-induced apoptosis, whereas turning it down increases the rate of *bax*-induced apoptosis.

We then performed the same experiments with *debcl*-expressing flies. As for *bax*-induced cell death, the $\Delta p54$ mutation was found to suppress *debcl*-induced apoptosis (figure 5, $\Delta p54C$ and T) whereas the *pros25*^{EP931} mutation enhanced this process (figure 5, *pros25*^{EP931} C and T, shows a shift from 31.4% strong phenotypes to 82.7%). The suppression of the *debcl*-induced phenotype by $\Delta p54$ is shown in figure 3 D-D' and the enhancement of this phenotype by *pros25*^{EP931} in figure 3 E-E'. Thus, the apoptotic processes induced by *Bax* and *Debcl* are regulated by proteasomal degradation. Moreover, as increasing the proteasomal activity suppresses the apoptosis induced by these two proteins whereas decreasing it enhances cell death, the regulator degraded in these processes is presumably a pro-apoptotic molecule.

The *Bax* and *Debcl* proteins are degraded by the proteasome

Some members of the Bcl-2 family in mammals are subject to proteasome-mediated regulation. We therefore hypothesized that *Bax* and *Debcl* proteins were the pro-apoptotic regulators degraded by the proteasome in our system. To test whether the modulation of *Bax*- and *Debcl*-induced cell death involves a direct effect on the level of these proteins, we performed immunostaining and western-blot experiments.

First, wing discs of *vg>bax* third-instar larvae were labeled with an anti-*Bax* antibody (figure 6A, *vg>bax*) revealing a strong staining in the region in which *vg* drove *gal4* expression (right part of figure 6A, *i.e.* *vg-gal4*-mediated expression of GFP). High-intensity foci correspond to cells overexpressing *bax*. The same

immunolabeling was performed on *vg>bax*, *Uba1^{EP2375}* wing discs, which coexpress *bax* and *Uba1*. Staining of Bax in *Uba1^{EP2375}*-expressing discs was weaker, with fewer foci of *bax* overexpressing cells (figure 6A, *vg>bax*, *Uba1^{EP2375}*). This suggests that Bax protein levels are lower in discs overexpressing *Uba1*. To confirm that the decrease in immunodetection of Bax, when *Uba1* is overexpressed, is due to a decrease in Bax levels and not a loss of epitope accessibility, we carried out a western blotting analysis.

To this purpose, we expressed *bax* or *debcl* ubiquitously in embryos, using the *da-gal4* driver with or without overexpressing *Uba1* from the *Uba1^{EP2375}* allele. We then carried out western blotting to determine the amounts of Bax or Debcl in embryo lysates. When *Uba1* was overexpressed (figure 6B, *da>bax*, *Uba1^{EP2375}*), Bax became undetectable, even after long exposure times, whereas this protein was readily detectable in the control extract (figure 6B, *da>bax*, control). Similarly, as shown figure 6C, *Uba1* overexpression resulted in a strong decrease in Debcl protein levels, as a longer exposure time was required to detect Debcl (data not shown). Moreover, although the amount of Debcl was decreased by *Uba1* overexpression, *Uba1* had no effect on the relative distribution of Debcl between cytosol and mitochondria. Debcl remained mainly detected in the mitochondrial fraction in the presence of *Uba1* overexpression (data not shown). We can therefore conclude that the ubiquitin-mediated regulation of Bax- and Debcl-induced cell death depended on a decrease in the level of Bax and Debcl proteins themselves.

The apoptotic processes induced by Bax and Debcl are regulated by an SCF^{Slmb} complex

As E3 ubiquitin ligases confer its specificity to the ubiquitination process, we tried to identify the E3 responsible for the regulation of *bax*- and *debcl*-induced cell death. Many signalization pathways involve SCF complexes. Thus, we first affected a common component to all SCF complexes SkpA. Overexpression of *skpA* using the *skpA^{EP1423}* allele under control of *vg-gal4* did not affect wing phenotypes. We thus overexpressed this allele in a *vg>bax* background. The progeny overexpressing both *bax* and *skpA*, displayed suppression of the *bax*-induced phenotype. The *skpA^{EP1423}* allele shifted the phenotype distribution toward weaker phenotypes (figure 4 *skpA^{EP1423}* C and T).

slmb (*supernumerary limb*) encodes an F-box protein homologous to mammalian β -TrCP, which is involved in Mcl-1 recognition in mammals. Slmb contains two functional domains: the F-box domain in the N-terminal half of the protein allowing assembling into the SCF complex through interaction with SkpA, and a C-terminal domain containing WD40 repeats, allowing interaction with substrates. We used *slmb⁸* -a null allele of *slmb* which is viable at 18°C (*i.e.* the temperature used for the *bax*-induced cell death phenotypic suppression tests)- and *slmb⁴¹* -a hypomorphic allele- to decrease the amount of Slmb (36). The *slmb⁸* loss-of-function allele strongly enhanced the *bax*-induced apoptosis-associated phenotype (figure 4 *slmb⁸* C and T). Indeed, strong phenotypes were significantly more frequent among the *slmb⁸* mutants than in the absence of this mutation. The *slmb⁴¹* allele also enhanced the *bax*-induced phenotype, although to a lesser extent (figure 4 *slmb⁴¹* C and T). Thus, Slmb most likely targets a pro-apoptotic regulator to proteasomal degradation in our system.

To investigate whether the same SCF^{Slmb} E3 ligase was involved in regulating *debcl*-induced cell death, we carried out the phenotypic test with *debcl*-expressing flies. We tested the effect of a loss-of-function of *slmb* on *debcl*-induced cell death as it is the specific component of the SCF complex. The *slmb⁸* mutant is partially lethal at 25°C (*i.e.* the temperature used for the *debcl*-induced cell death phenotypic suppression tests). We thus used the *slmb⁴¹* allele for these tests and observed higher levels of *debcl*-induced cell death. A shift in the phenotype distribution from 5% (*slmb⁴¹* C) to 50% of strong phenotypes (*slmb⁴¹* T) was observed (figure 5). This enhancement was characterized by an increase in size of the fusion of the L3 and L4 veins in the region of the anterior crossvein (figure 3 F-F'). Therefore the SCF^{Slmb} E3 ubiquitin ligase is a negative regulator of *bax*- and *debcl*-induced apoptosis.

Finally, as a control, we investigated whether *morgue* affected *bax*- and *debcl*-induced apoptosis. Like Slmb, Morgue is an F-box protein but it is involved in the regulation of apoptosis through the targeting of Diap1 for proteasomal degradation. The hypomorphic *morgue^{EP1184}* allele (40) had no effect on the phenotype induced by Bax or Debcl, as shown figure 3 G-G' for the *debcl*-induced crossvein phenotype. As indicated in figures 4 and 5, no significant change in phenotype distribution was observed in either case (α values of 7×10^{-3} for *bax* and 2.4×10^{-2} for *debcl*). We also verified that this allele did not affect fly phenotypes in presence of *vg-gal4* or *ptc-gal4* drivers alone. The lack of effect of *morgue* suggests that Morgue is not the F-box protein involved in our system. Hence, the effects observed with *slmb* alleles reflect specific Diap1-independent regulation.

Given that Debcl is sensitive to the proteasome activity and that a mutation of *slmb* enhances the *debcl*-induced cell death, we speculated that Debcl physically interacts with Slmb. We performed two types of experiments with the aim of characterizing this physical interaction. In agreement with genetic data, Debcl co-immunoprecipitates with Slmb (figure 7A). We assessed the occurrence of this physical interaction *in vivo* by using a proximity ligation *in situ* assay (figure 7B). Red dots are specifically observed in *Ptc>Debcl-HA, Slmb^{DN}-flag-myc* wing discs, indicating that Debcl and Slmb colocalize within 40 nm. This approach confirmed that the two proteins can interact with each other *in vivo*. Together with our genetic data, these results show that a SCF^{Slmb} E3 ubiquitin ligase is involved in Debcl ubiquitination and subsequent proteasomal degradation.

Discussion

In this paper, using *Drosophila* as a model for genetic studies, we report the regulation of *bax*- and *debcl*-induced apoptosis by the ubiquitin-proteasome pathway. The stimulation of this pathway by overexpressing *Uba1*, which encodes the ubiquitin activating enzyme, leads to an almost complete loss of *bax*-induced cell death. This regulation seems conserved through evolution, as *debcl*-induced apoptosis is also regulated in this way. However, since Bax seems to necessitate Debcl in order to kill *Drosophila* eye cells (25), one could wonder whether suppression of Bax-induced cell death depends on the direct effect of *Uba1* on Debcl. Nevertheless, since we have shown that both Bax and Debcl proteins are degraded when *Uba1* is overexpressed, this seems unlikely unless Debcl stabilizes Bax.

Since Buffy inhibits autophagy in response to starvation (41), we can hypothesize that Debcl could induce an autophagic cell death. We have monitored autophagy in our system by using a UAS-Atg8-GFP transgene (42) and found that actually no autophagy could be detected upon Debcl expression (data not shown). *Uba1* has been shown in the literature to be required for autophagy and reduction of cell size in the intestine (43). We show here that Debcl-induced cell death in the wing disc is not only suppressed by *Uba1* but also by proteasome mutants. These data suggest that the UPS pathway is the main proteolytic pathway involved in the suppression of Bax and Debcl-induced apoptosis by *Uba1*. However, given that *slmb* has been shown to regulate Wg and Dpp pathways (36, 44-46), we cannot exclude that these pathways are partially involved in phenotypic suppression.

Studies of the proteasome-dependent regulation of members of the Bcl-2 family in mammals have only rarely led to the identification of the specific E3 ligases. We identified an SCF^{Slmb} complex as the E3 ubiquitin ligase that regulates the Debcl pathway and may target it to proteasomal degradation. It would be interesting to determine whether the mammalian homologue of Slmb, β -TrCP, targets Bax to the proteasome in mammalian cells.

Here, we proved Debcl to be a target of the UPS, finding a new regulation of apoptosis that differs from the control of Dronc, Drice and RHG protein levels by Diap1. Indeed, Diap1 is a key enzyme that decides of cell fate by degrading either pro-apoptotic regulators or itself, leading to either cell survival or apoptosis. Since Diap1 levels are downregulated by the F-box protein Morgue in presence of Rpr or Grim, we could hypothesize that the Morgue/Diap1 pathway is involved in *bax*- and *debcl*-induced apoptosis regulation. This does not seem to be the case because a hypomorphic allele of *morgue* did not increase *bax*- and *debcl*-induced apoptosis (data not shown). Furthermore, overexpression of *diap1* does not inhibit *bax*- and *debcl*-induced apoptosis (data not shown). Thus, the proteasome-dependent regulation we identified is independent of Diap1 and differs from the Morgue/Diap1 regulation of cell death. The existence of different UPS-modulated cell death pathways is also supported by the reported absence of genetic interaction between RHG pathway components and Debcl (25).

Our results indicate an anti-apoptotic role of *Uba1* in the wing tissue. In contrast, two studies revealed a pro-apoptotic role of *Uba1* in the eye; strong *Uba1* loss-of-function alleles lead to apoptosis and compensatory proliferation in the developing eye (47, 48). As previously shown in other systems, these processes seem to involve the RHG/Diap1/Dronc pathway (49, 50). Hypomorphic alleles of *Uba1* have shown opposite effects as they suppressed *hid*- or *grim*-induced apoptosis in the eye. These results are consistent with previous data indicating that *Uba1* overexpression, using the *Uba1*^{EP2375} allele, increases RHG-induced apoptosis. In principle, this apparent contradiction may result from either the cell death signal or the studied tissue. The use of a GMR-Gal4 driver shows that *Uba1* overexpression also inhibits *debcl*-induced apoptosis in the eye tissue (data not shown), which suggests that the *Uba1* effect is specific of *debcl*-induced apoptosis. In contrast, *rpr*-induced cell death is enhanced by *Uba1* overexpression in the eye, whereas it is suppressed by *Uba1* in the wing (data not shown). These results suggest that Debcl could be involved in *rpr*-induced cell death in the wing but not in the eye. RHG proteins are known to mediate their pro-apoptotic function by stimulating Diap1 degradation by the UPS while Debcl is a direct target of ubiquitination. Therefore, RHG-induced degradation of Diap1 through its ubiquitination by Morgue could explain the pro-apoptotic role of *Uba1* in the eye whereas the anti-apoptotic *Uba1* function mediated by Slmb in Debcl-induced cell death would rely on Debcl degradation. By showing that different pro-apoptotic pathways are regulated by the UPS in *Drosophila*, our work suggests that the tissue-dependent effect of the pleiotropic enzyme *Uba1* must result from a change in the balance between UPS pro- and anti-apoptotic effects. We propose that this change relies on the availability in E3 enzymes, the incoming signals and relative amounts of pro- and anti-apoptotic regulators of cell fate.

Acknowledgments

We thank A. Udvardy for generously providing us with the $\Delta p54$ mutant and B. Limbourg-Bouchon and T. Murphy for the *slmb* mutants. We also thank Herman Steller and Tommaso Villa for critical reading of the manuscript. This work was supported by the Université de Versailles Saint-Quentin-en-Yvelines and by grants

1 from the *Association pour la Recherche Contre le Cancer* (#3819) and the *Ligue Nationale Contre le Cancer*
2 (*Comité des Yvelines*). Confocal microscopy was performed on CYMAGES imaging facility. Jessie Colin was
3 the recipient of a fellowship from *Ministère de la Recherche et de l'Enseignement Supérieur*. Jessie Colin and
4 Julie Garibal were supported by the *Ecole Pratique des Hautes Etudes*.
5

6 **References**

- 7 1. Estaquier J, Vallette F, Vayssiere JL, Mignotte B. (2012) The mitochondrial pathways of apoptosis. *Adv Exp*
8 *Med Biol* 942:157-183.
- 9 2. Zhong Q, Gao W, Du F, Wang X. (2005) Mule/ARF-BP1, a BH3-only E3 ubiquitin ligase, catalyzes the
10 polyubiquitination of Mcl-1 and regulates apoptosis. *Cell* 121:1085-1095.
- 11 3. Ding Q, He X, Hsu JM, et al. (2007) Degradation of Mcl-1 by beta-TrCP mediates glycogen synthase kinase
12 3-induced tumor suppression and chemosensitization. *Mol Cell Biol* 27:4006-4017.
- 13 4. Magiera MM, Mora S, Mojsa B, Robbins I, Lassot I, Desagher S. (2013) Trim17-mediated ubiquitination and
14 degradation of Mcl-1 initiate apoptosis in neurons. *Cell death and differentiation* 20:281-292.
- 15 5. Breitschopf K, Haendeler J, Malchow P, Zeiher AM, Dimmeler S. (2000) Posttranslational modification of
16 Bcl-2 facilitates its proteasome-dependent degradation: molecular characterization of the involved signaling
17 pathway. *Mol Cell Biol* 20:1886-1896.
- 18 6. Breitschopf K, Zeiher AM, Dimmeler S. (2000) Ubiquitin-mediated degradation of the proapoptotic active
19 form of bid. A functional consequence on apoptosis induction. *J Biol Chem* 275:21648-21652.
- 20 7. Akiyama T, Bouillet P, Miyazaki T, et al. (2003) Regulation of osteoclast apoptosis by ubiquitylation of
21 proapoptotic BH3-only Bcl-2 family member Bim. *Embo J* 22:6653-6664.
- 22 8. Li B, Dou QP. (2000) Bax degradation by the ubiquitin/proteasome-dependent pathway: involvement in
23 tumor survival and progression. *Proc Natl Acad Sci U S A* 97:3850-3855.
- 24 9. Liu FT, Agrawal SG, Gribben JG, et al. (2008) Bortezomib blocks Bax degradation in malignant B cells
25 during treatment with TRAIL. *Blood* 111:2797-2805.
- 26 10. Gardai SJ, Hildeman DA, Frankel SK, et al. (2004) Phosphorylation of Bax Ser184 by Akt regulates its
27 activity and apoptosis in neutrophils. *J Biol Chem* 279:21085-21095.
- 28 11. Tsuruta F, Masuyama N, Gotoh Y. (2002) The phosphatidylinositol 3-kinase (PI3K)-Akt pathway suppresses
29 Bax translocation to mitochondria. *J Biol Chem* 277:14040-14047.
- 30 12. Xin M, Deng X. (2005) Nicotine inactivation of the proapoptotic function of Bax through phosphorylation. *J*
31 *Biol Chem* 280:10781-10789.
- 32 13. Xin M, Gao F, May WS, Flagg T, Deng X. (2007) Protein Kinase C{zeta} Abrogates the Proapoptotic
33 Function of Bax through Phosphorylation. *J Biol Chem* 282:21268-21277.
- 34 14. Amsel AD, Rathaus M, Kronman N, Cohen HY. (2008) Regulation of the proapoptotic factor Bax by Ku70-
35 dependent deubiquitylation. *Proc Natl Acad Sci U S A* 105:5117-5122.
- 36 15. Quinn L, Coombe KM, Tasman D, Colussi P, Kumar S, Richardson H. (2003) Buffy, a *Drosophila* Bcl-2
37 protein, has anti-apoptotic and cell cycle inhibitory functions. *EMBO J* 22:3568-3579.
- 38 16. Sevrioukov EA, Burr J, Huang EW, et al. (2007) *Drosophila* Bcl-2 proteins participate in stress-induced
39 apoptosis, but are not required for normal development. *Genesis* 45:184-193.
- 40 17. Senoo-Matsuda N, Igaki T, Miura M. (2005) Bax-like protein Drob-1 protects neurons from expanded
41 polyglutamine-induced toxicity in *Drosophila*. *Embo J* 24:2700-2713.
- 42 18. Wu JN, Nguyen N, Aghazarian M, et al. (2010) grim promotes programmed cell death of *Drosophila*
43 microchaete glial cells. *Mechanisms of development* 127:407-417.
- 44 19. Tanner EA, Blute TA, Brachmann CB, McCall K. (2011) Bcl-2 proteins and autophagy regulate
45 mitochondrial dynamics during programmed cell death in the *Drosophila* ovary. *Development* 138:327-338.
- 46 20. Yacobi-Sharon K, Namdar Y, Arama E. (2013) Alternative germ cell death pathway in *Drosophila* involves
47 HtrA2/Omi, lysosomes, and a caspase-9 counterpart. *Developmental cell* 25:29-42.
- 48 21. Colussi PA, Quinn LM, Huang DC, et al. (2000) Debcl, a proapoptotic Bcl-2 homologue, is a component of
49 the *Drosophila melanogaster* cell death machinery. *J Cell Biol* 148:703-714.
- 50 22. Igaki T, Kanuka H, Inohara N, et al. (2000) Drob-1, a *Drosophila* member of the bcl-2/CED-9 family that
51 promotes cell death. *Proc Natl Acad Sci USA* 97:662-667.
- 52 23. Brachmann CB, Jassim OW, Wachsmuth BD, Cagan RL. (2000) The *Drosophila bcl-2* family member
53 dBorg-1 functions in the apoptotic response to UV-irradiation. *Curr Biol* 10:547-550.
- 54 24. Zhang H, Huang Q, Ke N, et al. (2000) *Drosophila* pro-apoptotic Bcl-2/Bax homologue reveals evolutionary
55 conservation of cell death mechanisms. *J Biol Chem* 275:27303-27306.
- 56 25. Galindo KA, Lu WJ, Park JH, Abrams JM. (2009) The Bax/Bak ortholog in *Drosophila*, Debcl, exerts limited
57 control over programmed cell death. *Development* 136:275-283.
- 58 26. Xu D, Li Y, Arcaro M, Lackey M, Bergmann A. (2005) The CARD-carrying caspase Dronc is essential for
59 most, but not all, developmental cell death in *Drosophila*. *Development* 132:2125-2134.
- 60
- 61
- 62
- 63
- 64
- 65

27. Goyal L, McCall K, Agapite J, Hartweg E, Steller H. (2000) Induction of apoptosis by *Drosophila* reaper, hid and grim through inhibition of IAP function. *Embo J* 19:589-597.
28. Lisi S, Mazzon I, White K. (2000) Diverse domains of THREAD/DIAP1 are required to inhibit apoptosis induced by REAPER and HID in *Drosophila*. *Genetics* 154:669-678.
29. Igaki T, Yamamoto-Goto Y, Tokushige N, Kanda H, Miura M. (2002) Down-regulation of DIAP1 triggers a novel *Drosophila* cell death pathway mediated by Dark and DRONC. *J Biol Chem* 277:23103-23106.
30. Colin J, Gaumer S, Guenal I, Mignotte B. (2009) Mitochondria, Bcl-2 family proteins and apoptosomes: of worms, flies and men. *Front Biosci* 14:4127-4137.
31. Gaumer S, Guenal I, Brun S, Theodore L, Mignotte B. (2000) Bcl-2 and Bax mammalian regulators of apoptosis are functional in *Drosophila*. *Cell death and differentiation* 7:804-814.
32. Brun S, Rincheval V, Gaumer S, Mignotte B, Guenal I. (2002) reaper and bax initiate two different apoptotic pathways affecting mitochondria and antagonized by bcl-2 in *Drosophila*. *Oncogene* 21:6458-6470.
33. Colin J, Garibal J, Mignotte B, Guenal I. (2009) The mitochondrial TOM complex modulates bax-induced apoptosis in *Drosophila*. *Biochem Biophys Res Commun* 379:939-943.
34. Monnier V, Girardot F, Cheret C, Andres O, Tricoire H. (2002) Modulation of oxidative stress resistance in *Drosophila melanogaster* by gene overexpression. *Genesis* 34:76-79.
35. Colussi PA, Quinn LM, Huang DC, et al. (2000) Debcl, a proapoptotic Bcl-2 homologue, is a component of the *Drosophila melanogaster* cell death machinery. *J Cell Biol* 148:703-714.
36. Miletich I, Limbourg-Bouchon B. (2000) *Drosophila* null slimb clones transiently deregulate Hedgehog-independent transcription of wingless in all limb discs, and induce decapentaplegic transcription linked to imaginal disc regeneration. *Mech Dev* 93:15-26.
37. Szlanka T, Haracska L, Kiss I, et al. (2003) Deletion of proteasomal subunit S5a/Rpn10/p54 causes lethality, multiple mitotic defects and overexpression of proteasomal genes in *Drosophila melanogaster*. *J Cell Sci* 116:1023-1033.
38. Wing JP, Schreuder BA, Yokokura T, et al. (2002) *Drosophila* Morgue is an F box/ubiquitin conjugase domain protein important for grim-reaper mediated apoptosis. *Nat Cell Biol* 4:451-456.
39. Neuburger PJ, Saville KJ, Zeng J, Smyth KA, Belote JM. (2006) A genetic suppressor of two dominant temperature-sensitive lethal proteasome mutants of *Drosophila melanogaster* is itself a mutated proteasome subunit gene. *Genetics* 173:1377-1387.
40. Wing JP, Schreuder BA, Yokokura T, et al. (2002) *Drosophila* Morgue is an F box/ubiquitin conjugase domain protein important for grim-reaper mediated apoptosis. *Nat Cell Biol* 4:451-456.
41. Monserrate JP, Chen MY, Brachmann CB. (2012) *Drosophila* larvae lacking the bcl-2 gene, buffy, are sensitive to nutrient stress, maintain increased basal target of rapamycin (Tor) signaling and exhibit characteristics of altered basal energy metabolism. *BMC biology* 10:63.
42. Mohseni N, McMillan SC, Chaudhary R, Mok J, Reed BH. (2009) Autophagy promotes caspase-dependent cell death during *Drosophila* development. *Autophagy* 5:329-338.
43. Chang TK, Shrivastava BV, Hayes SD, et al. (2013) Uba1 functions in Atg7- and Atg3-independent autophagy. *Nature cell biology* 15:1067-1078.
44. Muzzopappa M, Wappner P. (2005) Multiple roles of the F-box protein Slimb in *Drosophila* egg chamber development. *Development* 132:2561-2571.
45. Swarup S, Verheyen EM. (2011) *Drosophila* homeodomain-interacting protein kinase inhibits the Skp1-Cul1-F-box E3 ligase complex to dually promote Wingless and Hedgehog signaling. *Proceedings of the National Academy of Sciences of the United States of America* 108:9887-9892.
46. Theodosiou NA, Zhang S, Wang WY, Xu T. (1998) slimb coordinates wg and dpp expression in the dorsal-ventral and anterior-posterior axes during limb development. *Development* 125:3411-3416.
47. Lee TV, Ding T, Chen Z, et al. (2008) The E1 ubiquitin-activating enzyme Uba1 in *Drosophila* controls apoptosis autonomously and tissue growth non-autonomously. *Development* 135:43-52.
48. Pflieger CM, Harvey KF, Yan H, Hariharan IK. (2007) Mutation of the Gene Encoding the Ubiquitin Activating Enzyme Uba1 Causes Tissue Overgrowth in *Drosophila*. *Fly* 1:95-105.
49. Huh JR, Guo M, Hay BA. (2004) Compensatory proliferation induced by cell death in the *Drosophila* wing disc requires activity of the apical cell death caspase Dronc in a nonapoptotic role. *Curr Biol* 14:1262-1266.
50. Ryoo HD, Gorenc T, Steller H. (2004) Apoptotic cells can induce compensatory cell proliferation through the JNK and the Wingless signaling pathways. *Dev Cell* 7:491-501.

Figure legends

Figure 1. *vg-gal4*-mediated induction of the *UY3010* mutation significantly suppresses the *bax*-induced phenotype

1 (A) w^{1118} wild-type adult wing. (B-D) wings of $vg>bax$ flies. bax expression leads to phenotypes that fall into
2 three categories: weak (B), intermediate (C) and strong (D). Most specimens show strong or intermediate
3 phenotypes (adapted from (32)). (E) Distribution of the offspring between the strong, intermediate and weak
4 phenotype categories in $vg>bax$ and $vg>bax/Uba1^{UY3010}$ flies.
5

6 **Figure 2.** $Uba1^{EP2375}$ overexpression efficiently suppresses bax -induced apoptosis

7 (A, B) $vg>bax/Uba1^{EP2375}$ flies. $Uba1$ overexpression leads to the appearance of wild-type (A) or very weak
8 phenotypes, with only a small notch (B). (C) Distribution of the offspring between the strong, intermediate and
9 weak phenotype categories in $vg>bax$ and $vg>bax/Uba1^{EP2375}$ flies.
10 (D, F) Acridine orange stainings on third-instar larval leg (asterisks) and wing (arrowheads) discs expressing bax
11 in imaginal wing discs under control of the $vg-gal4$ driver ($vg>bax$) or coexpressing bax and $Uba1$ ($vg>bax +$
12 $Uba1^{EP2375}$). (E, G) Nomarsky views of the upper panels discs.
13
14
15

16 **Figure 3.** Wings from $debcl$ -expressing flies

17 (A-G) Adult wings and (A'-G') magnification of (A-G). (A, A') wild-type fly. (B, B') control fly of $ptc-$
18 $gal4,UAS-debcl/+;UAS-debcl/+$ genotype. (C, C') $ptc-gal4, UAS-debcl/Uba1^{EP2375};UAS-debcl/+$. (D, D')
19 $ptc-gal4,UAS-debcl/+;UAS-debcl/\Delta p54$. (E, E') $ptc-gal4,UAS-debcl/+;UAS-debcl/pros25^{EP931}$. (F, F') $ptc-$
20 $gal4,UAS-debcl/+;UAS-debcl/slmb^{41}$. (G, G') $ptc-gal4, UAS-debcl/morgue^{EP1184};UAS-debcl/+$. (H)
21 Distribution of the offspring between the strong, intermediate weak and wild type phenotype categories in
22 $ptc>debcl$ and $ptc>debcl/Uba1^{EP2375}$ flies.
23
24

25 **Figure 4.** Modulation of bax -induced wing phenotype

26 (A) Distribution of the offspring between the strong, intermediate and weak phenotype categories. Each bar
27 represents the progeny of a cross between $vg>bax$ flies and a control (C) or a mutant (T) strain. Each cross (T) is
28 presented with its control (C) that takes into account the specific genetic background of the tested strain. The
29 percentage of phenotypes in each category is shown on the y-axis. (B) Every phenotypic test was validated by
30 the statistical Wilcoxon test. The phenotype distribution of each test cross was compared with that of the
31 corresponding control. Differences in distribution with a probability $\alpha < 10^{-3}$ were considered significant; $Ws < 0$
32 indicates phenotype suppression and $Ws > 0$ indicates phenotype enhancement; n is the number of flies counted.
33
34
35

36 **Figure 5.** Modulation of $debcl$ -induced wing phenotype

37 (A) Distribution of offspring between the strong, intermediate and weak phenotype categories. Each bar
38 represents the progeny of a cross between $ptc>(debcl)_2$ flies and a control strain (C) or a mutant strain (T). Each
39 cross (T) is presented with its control (C). The percentage of phenotypes in each category is shown on the y-axis.
40 (B). Every phenotypic test was validated by carrying out a Wilcoxon test as in figure 4.
41
42
43
44

45 **Figure 6.** $Uba1$ controls the level of Bax and Debcl proteins

46 (A) Bax immunostaining on third-instar larval wing discs expressing bax under control of the $vg-gal4$ driver
47 ($vg>bax$) or coexpressing bax and $Uba1$ ($vg>bax + Uba1^{EP2375}$). The panel on the right shows GFP expression
48 driven by $vg-gal4$ in the wing pouch, along the dorso-ventral frontier. (B) Immunodetection of Bax in a $Uba1$
49 overexpression background. $Uba1$ decreases Bax protein quantities down to an undetectable level. (C)
50 Immunostaining of Debcl in a $Uba1$ overexpression background. $Uba1$ reduces the amount of Debcl protein. (B,
51 C) Immunodetection of tubulin was used as control.
52
53

54 **Figure 7.** $Debcl$ and $Slmb$ physically interact *in vivo*

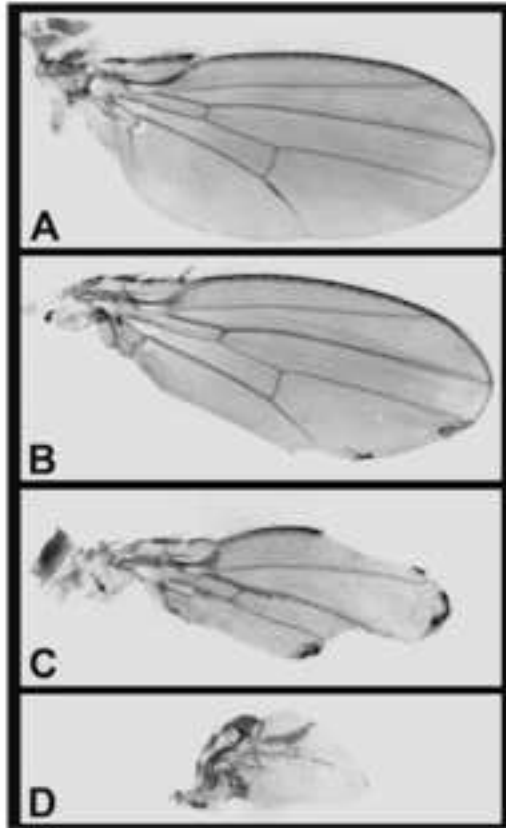
55 (A) Embryos ubiquitously co-expressing $Slmb^{DN}$ -flag-myc and $Debcl$ -HA ($UAS-debcl-HA/+; da>slmb^{DN}$ -flag-
56 $myc/UAS-debcl-HA$) were prepared as described in "Materials & Methods" and subjected to
57 immunoprecipitation (IP) with mouse anti-flag antibodies ($Slmb$) or IgG1 control (Irr). Western-blot analysis
58 was then performed with an anti-myc mAb ($Slmb$) or anti-HA mAb ($Debcl$). The input lane contains 6% of the
59 lysate while immunoprecipitates were obtained from 28% of the lysate. $Debcl$ co-immunoprecipitates with $Slmb$.
60 (B) Wing discs of $Ptc>Debcl-HA,Slmb^{DN}$ -flag-myc and $Ptc>Debcl-HA,Pabp$ -flag third instar larvae were
61
62
63
64
65

analysed by use of the proximity ligation *in situ* assay to monitor the Debcl/Slmb interaction. As expected, no signal was observed in *Ptc>Debcl-HA,Pabp-flag* discs whereas the red dots observed in *Ptc>Debcl-HA,Slmb^{DN}-flag-myc* indicate Slmb/Debcl colocalization.

1
2
3
4
5
6
7
8
9
10
11
12
13
14
15
16
17
18
19
20
21
22
23
24
25
26
27
28
29
30
31
32
33
34
35
36
37
38
39
40
41
42
43
44
45
46
47
48
49
50
51
52
53
54
55
56
57
58
59
60
61
62
63
64
65

Figure 1

[Click here to download high resolution image](#)



E

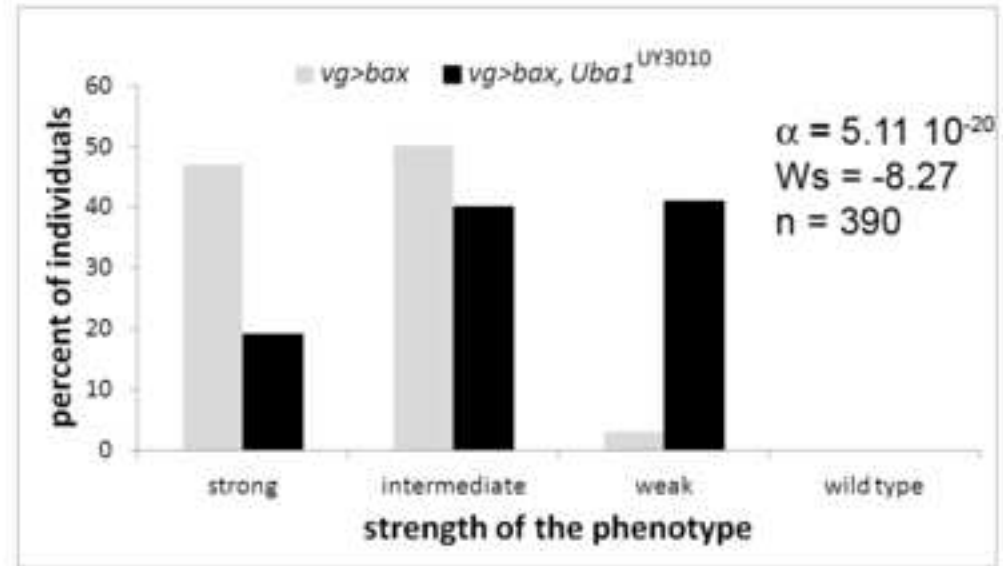


Figure 2

[Click here to download high resolution image](#)

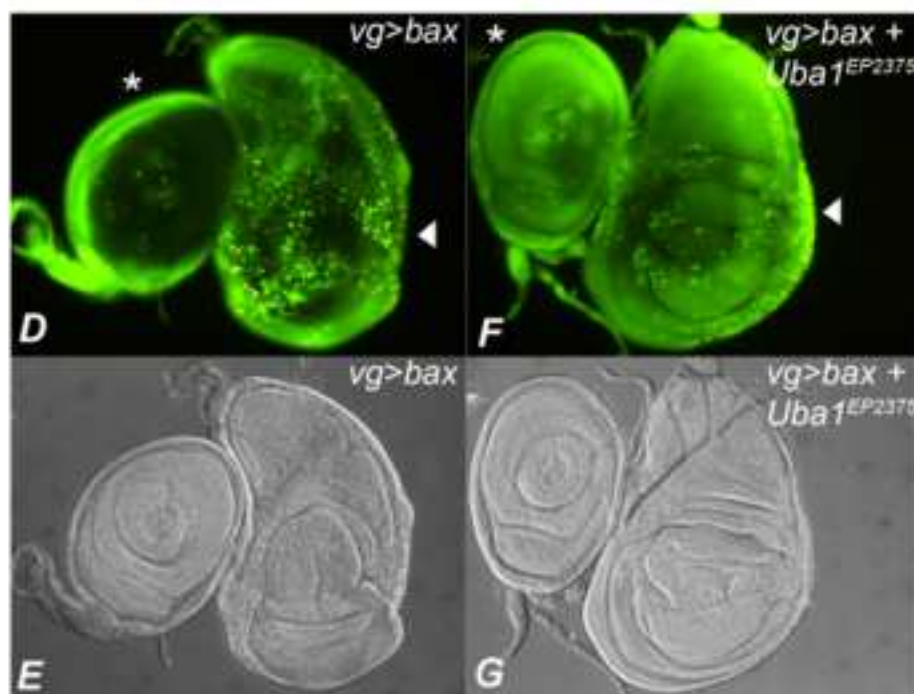
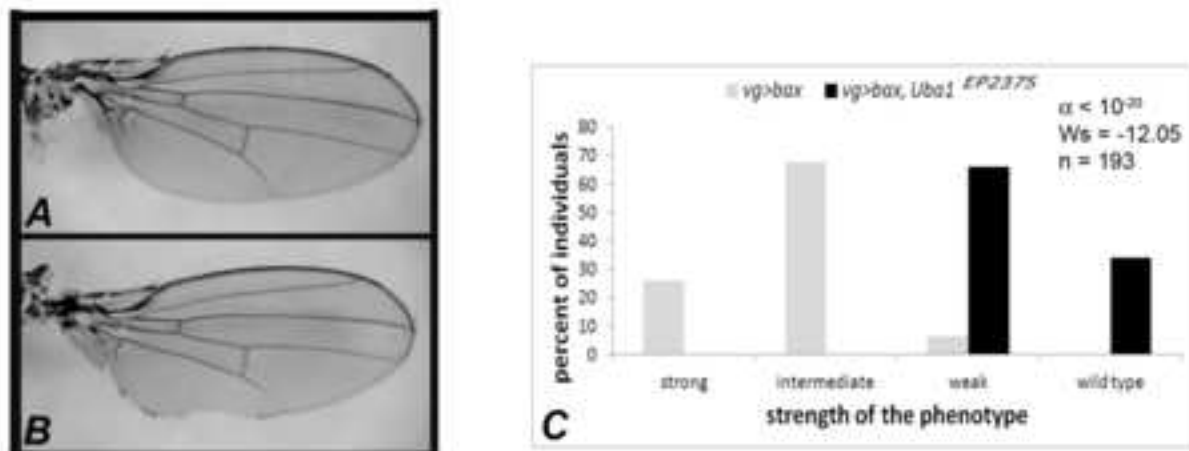
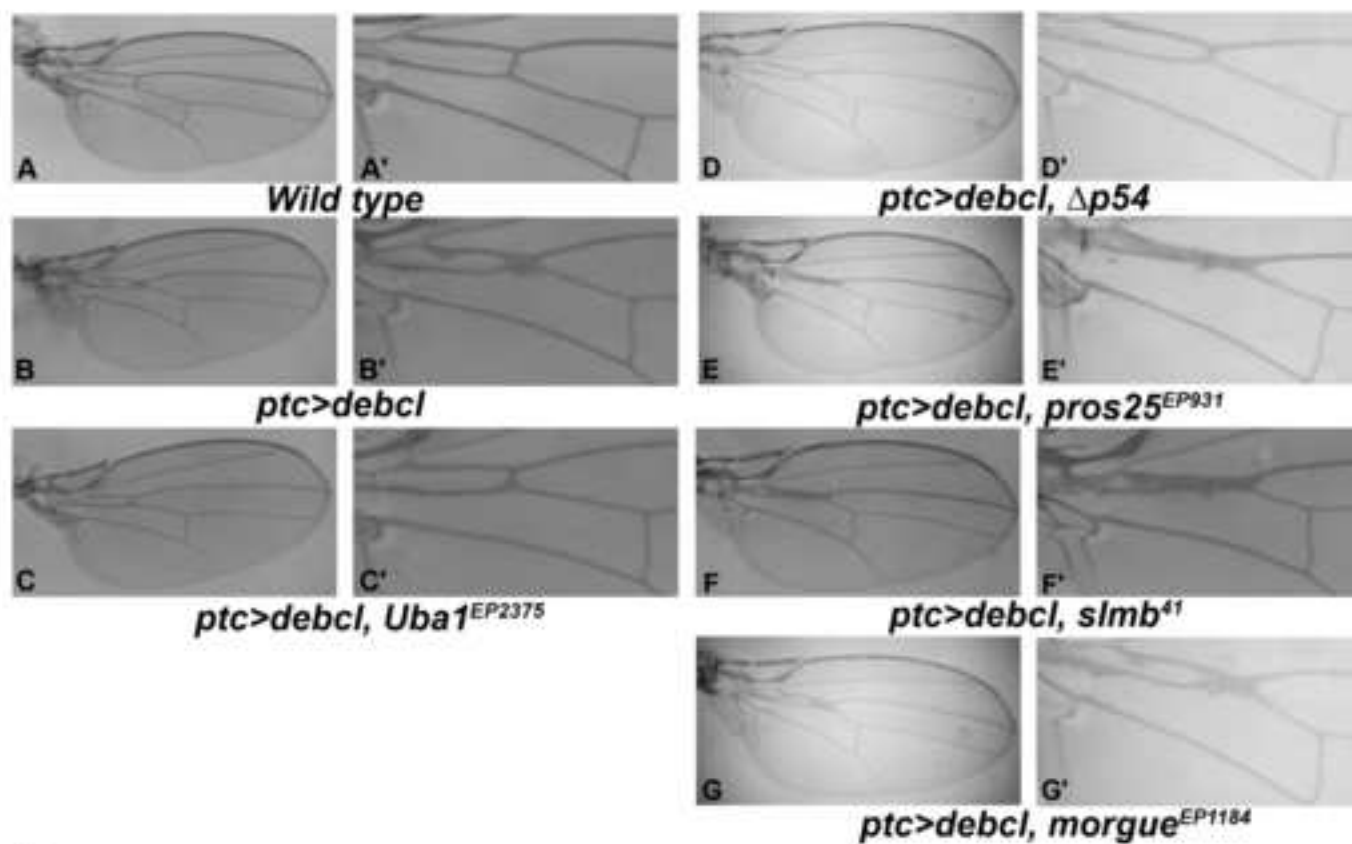


Figure 3

[Click here to download high resolution image](#)



H

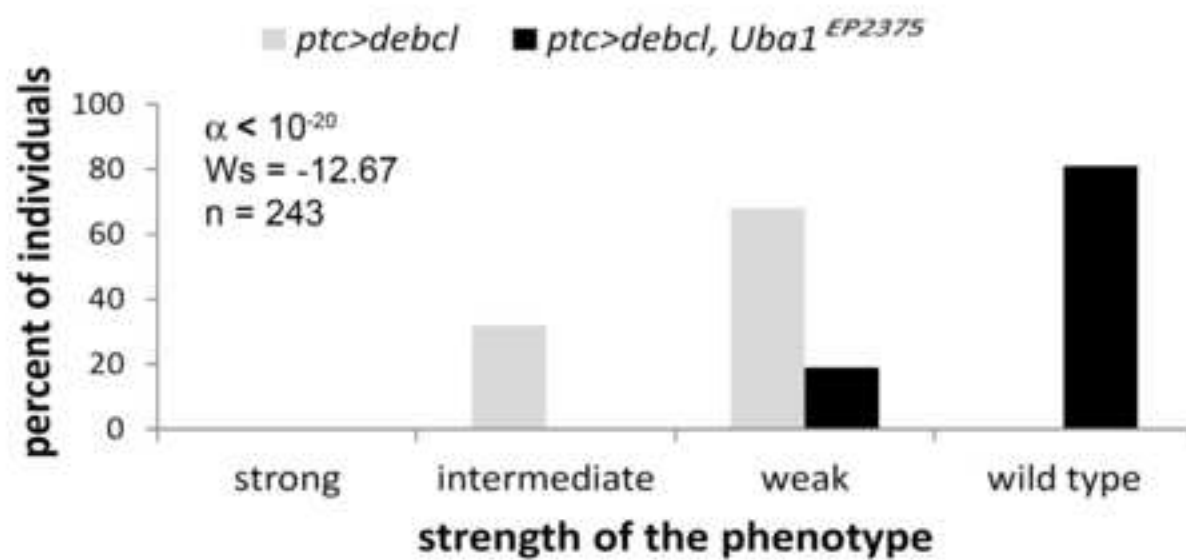
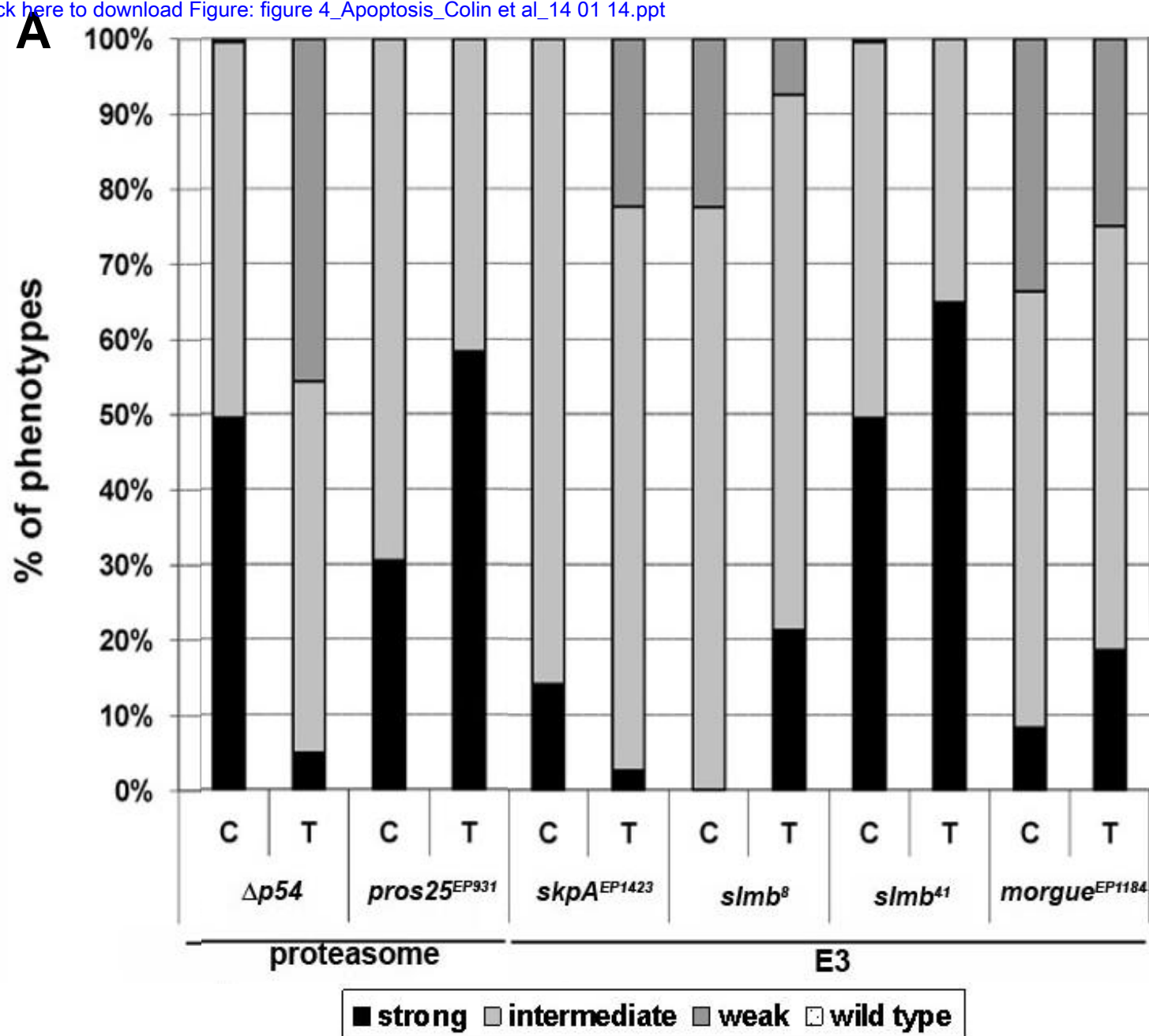


Figure 4

[Click here to download Figure: figure 4_Apoptosis_Colin et al_14 01 14.ppt](#)

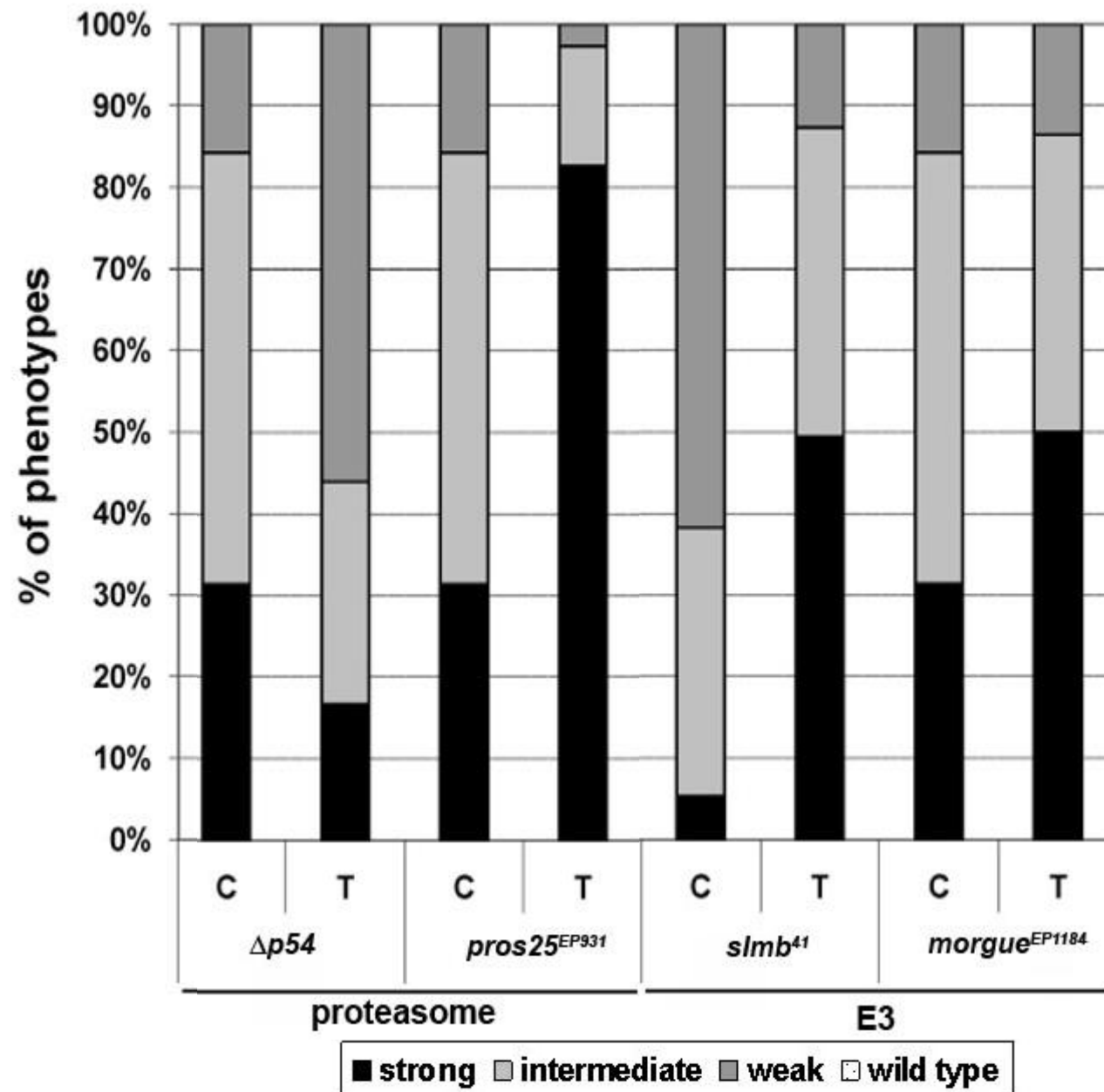


B

	<i>Δp54</i>	<i>pros25^{EP931}</i>	<i>skpA^{EP1423}</i>	<i>slmb⁸</i>	<i>slmb⁴¹</i>	<i>morgue^{EP1184}</i>
α	0	3.21×10^{-5}	1.68×10^{-7}	2.08×10^{-7}	1.24×10^{-3}	7.22×10^{-3}
Ws	-14.30	4.17	-5.30	5.25	3.23	2.69
n	578	272	190	236	542	349

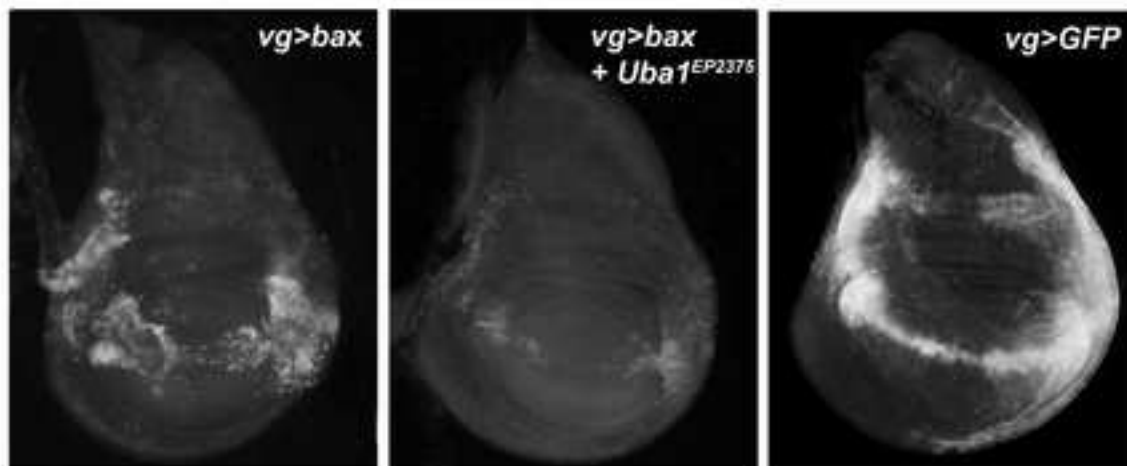
Figure 5

[Click here to download Figure: figure 5_Apoptosis_Colin et al_14 01 14.ppt](#)

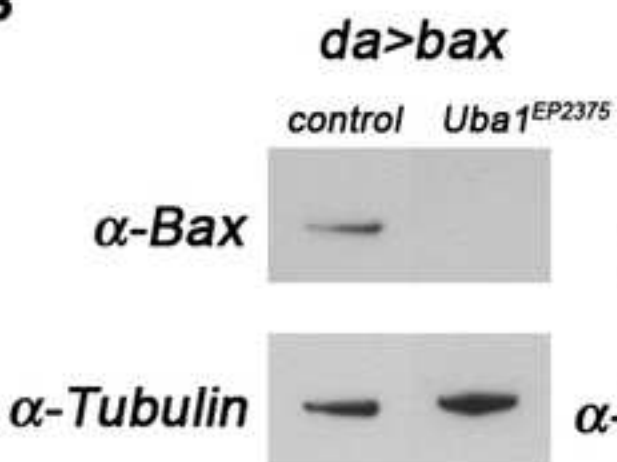
A**B**

	$\Delta p54$	$pros25^{EP931}$	$slmb^{41}$	$morgue^{EP1184}$
α	2.29×10^{-9}	1.69×10^{-11}	8.50×10^{-14}	0.024
Ws	-6.11	6.965	7.83	2.25
n	272	215	181	214

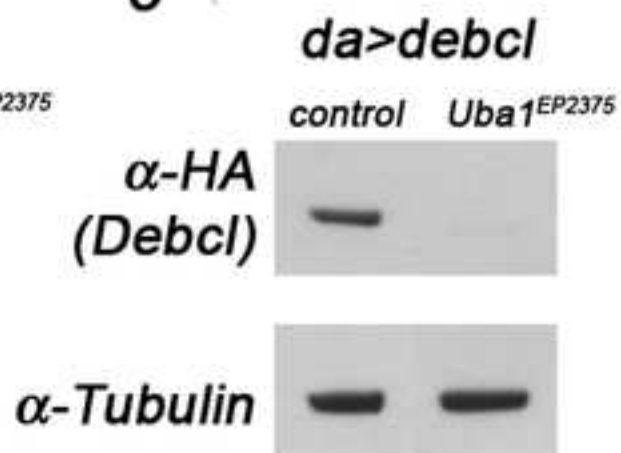
A

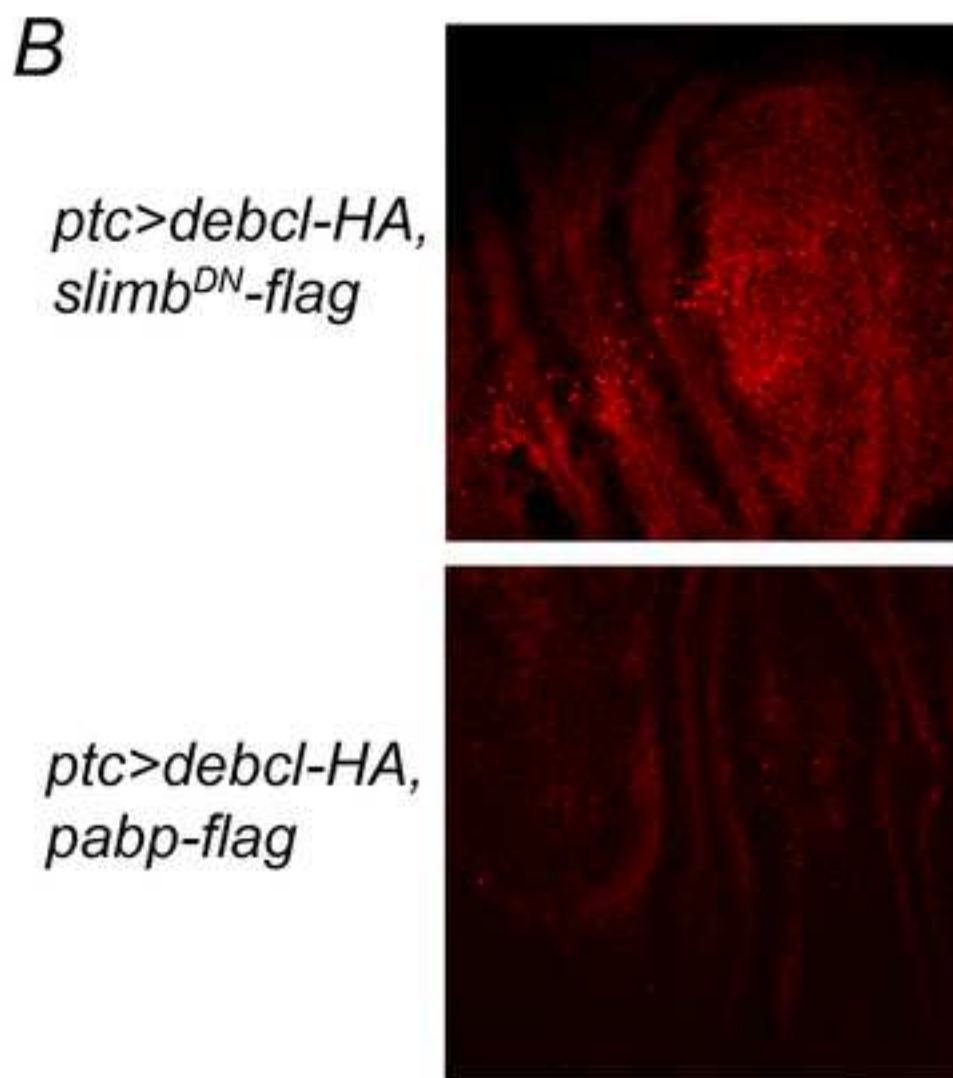
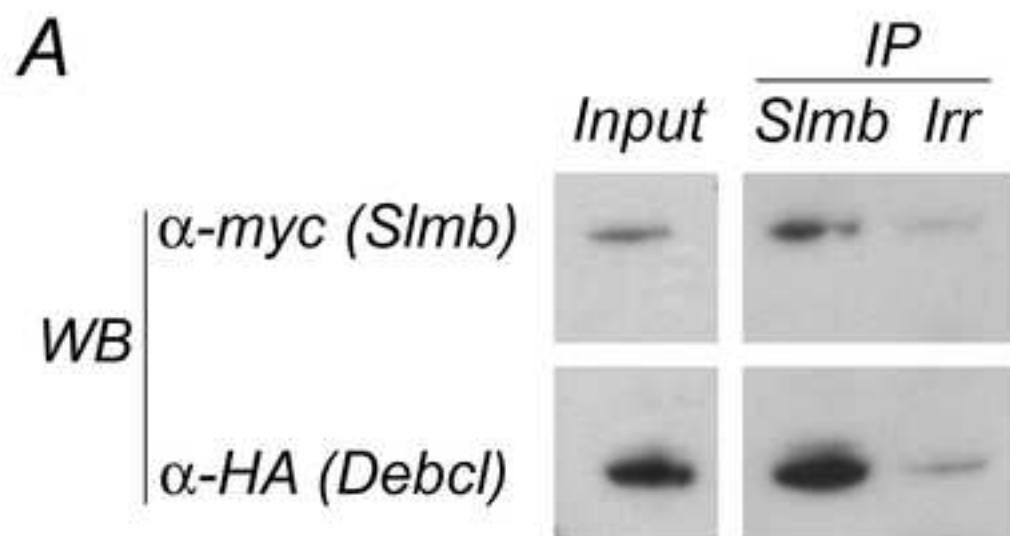


B



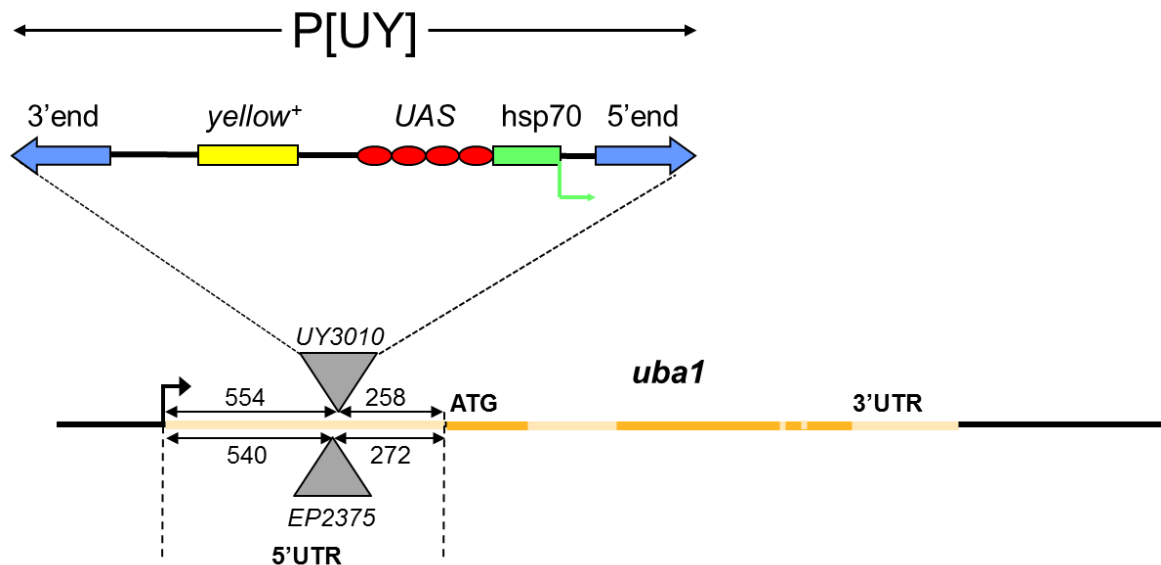
C





The *Drosophila* Bcl-2 family protein *Debcl* is targeted to the proteasome by the β -TrCP homologue *Slimb*

Jessie Colin, Julie Garibal, Amandine Clavier, Aurore Rincheval-Arnold, Sébastien Gaumer, Bernard Mignotte and Isabelle Guéna



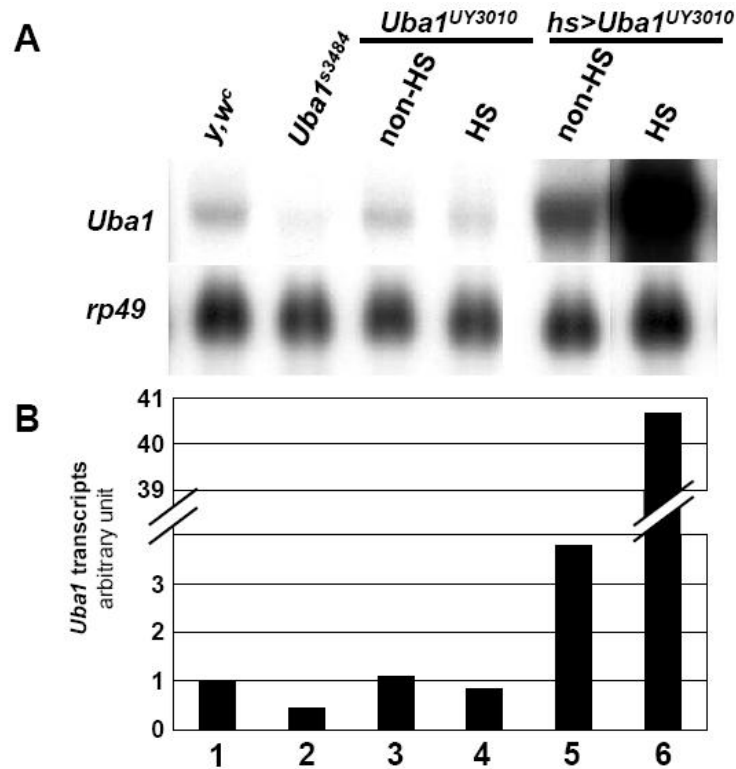
Supplementary figure 1

In the *UY3010* line, P[UY] is inserted in the 5'UTR region of *Uba1*.

Schematic diagram of the P[UY] insertion in the *UY3010* mutant. P[UY] is inserted in the 5'UTR region, 258 bp upstream from the start codon and 554 bp downstream from the transcription start site of the *Uba1* gene. The orientation of P[UY] is compatible with UAS-mediated *Uba1* overexpression in the presence of Gal4. The insertion of the P[EP] in the *Uba1*^{EP2375} line is 272 bp upstream from the start codon and also compatible with UAS-mediated *Uba1* overexpression.

The Drosophila Bcl-2 family protein Debcl is targeted to the proteasome by the β -TrCP homologue Slimb

Jessie Colin, Julie Garibal, Amandine Clavier, Aurore Rincheval-Arnold, Sébastien Gaumer, Bernard Mignotte and Isabelle Guénael



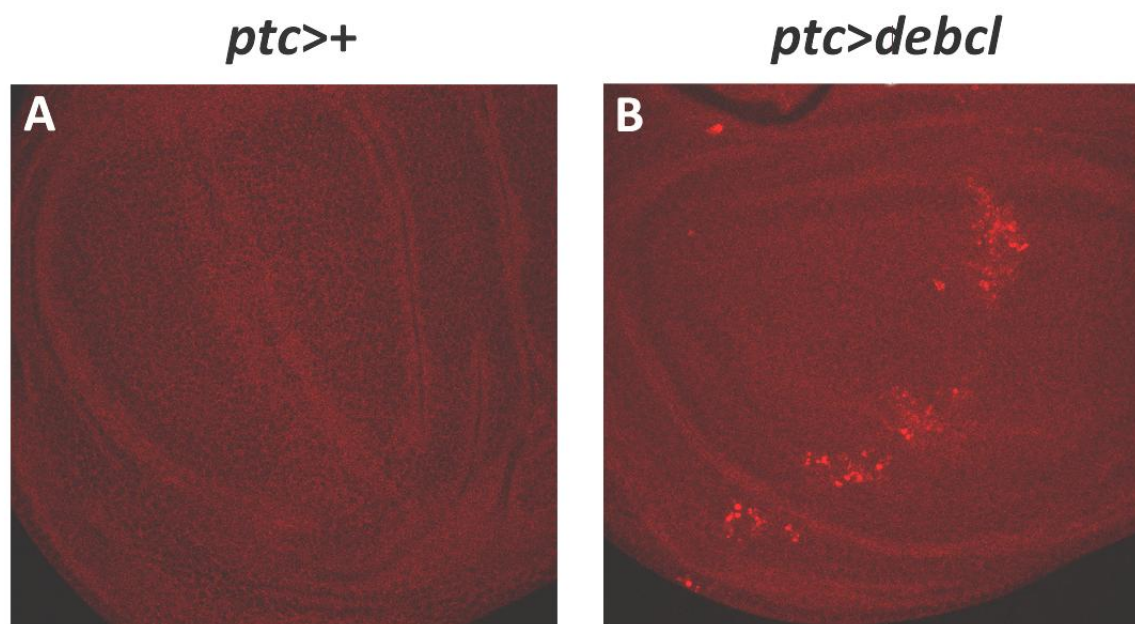
Supplementary figure 2

Uba1^{UY3010} can be used to overexpress *Uba1* under *gal4* induction.

(A) Northern blot on total RNA from adult flies. Genotype of flies: *y,w^c*: wild-type; *Uba1^{s3484}*. *Uba1^{s3484}/CyO* (loss-of-function allele of *Uba1*), *Uba1^{UY3010}*. *Uba1^{UY3010}/CyO*; *hs>Uba1^{UY3010}*: *hs-gal4,Uba1^{UY3010}/CyO*. Flies were subjected to heat shock treatment (HS) or not (non-HS). We used probes specific for *Uba1* (top) or *rp49* (bottom) as a control. (B) Quantification of *Uba1* transcripts. *Uba1* transcript levels were normalized with respect to *rp49*, with wild-type *Uba1* transcript (*y,w^c*) levels set at 1. The loss-of-function allele of *Uba1*, *Uba1^{s3484}*, had half as many *Uba1* transcripts as the wild-type. Use of the *hs-gal4* driver and *Uba1^{UY3010}* led to a 10 times increase in *Uba1* transcript levels in response to heat shock treatment.

The *Drosophila* Bcl-2 family protein *Debcl* is targeted to the proteasome by the β -TrCP homologue *Slimb*

Jessie Colin, Julie Garibal, Amandine Clavier, Aurore Rincheval-Arnold, Sébastien Gaumer, Bernard Mignotte and Isabelle Guénaï



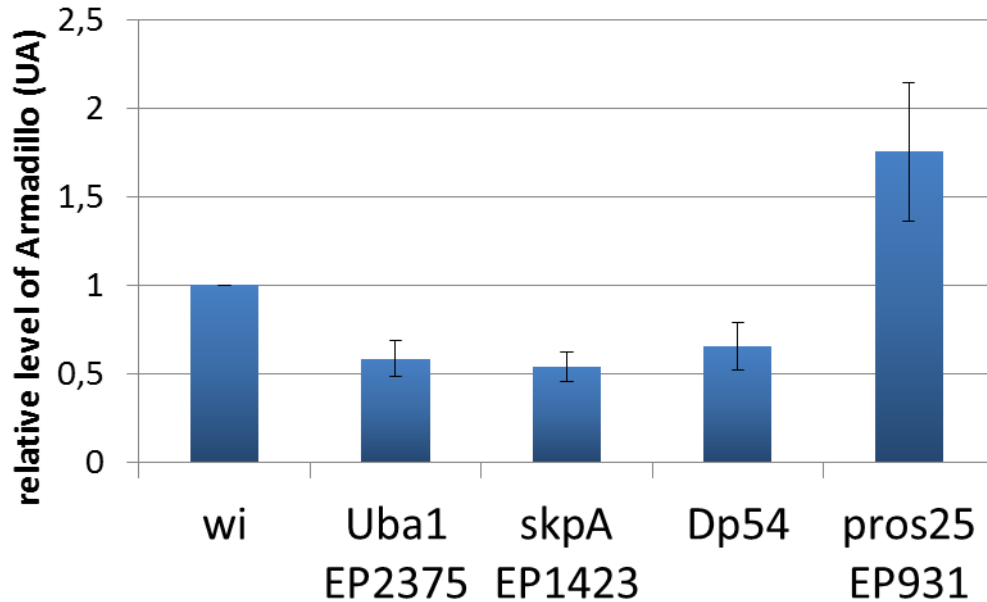
Supplementary figure 3

Expression of *UAS-debcl* in the wing imaginal disc thanks to the *ptc-gal4* driver induces apoptosis along the antero-posterior frontier

Apoptotic cells were visualized by TUNEL staining of wing imaginal discs of the genotype indicated at the top of the image.

The *Drosophila* Bcl-2 family protein Debcl is targeted to the proteasome by the β -TrCP homologue Slimb

Jessie Colin, Julie Garibal, Amandine Clavier, Aurore Rincheval-Arnold, Sébastien Gaumer, Bernard Mignotte and Isabelle Guéna



Supplementary figure 4

Effects of mutations on proteasome activity.

Cell lysates from *Drosophila* head of w^{1118} (wi), GMR-Gal4>Uba1^{EP2375}, GMR-Gal4>skpA^{EP1423}, Dp54 and GMR-Gal4>pros25^{EP931} flies were migrated on PAGE and probed with anti-armadillo (N2 7A1 from DSHB, 1/500) and anti-tubulin (E7 from DSHB, 1/1000) antibodies. Armadillo levels were normalized with tubulin levels and the ratio was set to 1 for wi flies. Results were from at least 3 independent experiments per genotype.

The *Drosophila* Bcl-2 family protein *Debcl* is targeted to the proteasome by the β -TrCP homologue *Slimb*

Jessie Colin, Julie Garibal, Amandine Clavier, Aurore Rincheval-Arnold, Sébastien Gaumer, Bernard Mignotte and Isabelle Guénael

Supplementary methods

Heat-shock treatment

Young males were placed in empty tubes at 36°C for 45 minutes. They were then transferred to a tube containing standard medium and incubated at 21°C for one day. This temperature shift was repeated 24 hours later. Flies were finally recovered five hours after heat shock and RNA was extracted.

Northern blot

Total RNA was extracted from 25 males by homogenization in Trizol (Life Technologies, phenol and guanidine isothiocyanate) and precipitated in isopropanol. The RNA was resuspended in water and its concentration evaluated by spectrophotometry (OD 260/280 nm). Northern blotting was then carried out with 30 μ g of total RNA, using standard methods. The probes specific for *Uba1* or *rp49* (ribosomal protein, control for quantification), were generated by PCR, using the following primers:

5'-GTGTATTCCGACCAGGTTACA-3' (*rp49*, forward primer)

5'-ATACAGGCCCAAGATCGTGA-3' (*rp49*, reverse primer)

5'-TGTCGTCGCAATTCTATCTCAC-3' (*Uba1*, forward primer)

5'-TGGCAATCTGAGAATGATAGCC-3' (*Uba1*, reverse primer)

These probes were obtained by random priming and polymerization with the Klenow fragment of DNA polymerase I. The radioactive nucleotide used was α dCTP³². Quantification was achieved with a phosphorimager and normalized with respect to *rp49*.

TUNEL staining of wing imaginal discs

Discs were dissected and TUNEL staining was performed according to manufacturer's instructions (ApopTag® Red in situ apoptosis detection kit, Chemicon). Discs were mounted in Citifluor™ (Biovalley) and observed with a Leica SPE upright confocal microscope with an x63 objective.